

Original Research Article

Exploring Lumacaftor: a novel antibacterial approach for treating *E. coli*-induced urinary tract infections

Anjali G.¹, Lakshmi M.¹, Deepika Srija B.¹, Ushaswini M.¹, Neeraja K.¹, Venkateswarlu T.C.², Anuradha V.³, Meenakshi Kante^{1*}

¹Department of Microbiology, Vignan P. G. College, Guntur, Andhra Pradesh, India

²Department of Biotechnology and Bioinformatics, Vignan University, Guntur, Andhra Pradesh, India

³Department of Chemistry, Vignan P. G. College, Guntur, Andhra Pradesh, India

Received: 28 May 2025

Revised: 04 July 2025

Accepted: 23 July 2025

*Correspondence:

Dr. Meenakshi Kante,

E-mail: meena.apple86@gmail.com

Copyright: © the author(s), publisher and licensee Medip Academy. This is an open-access article distributed under the terms of the Creative Commons Attribution Non-Commercial License, which permits unrestricted non-commercial use, distribution, and reproduction in any medium, provided the original work is properly cited.

ABSTRACT

Background: Urinary tract infections (UTIs) are primarily caused by *Escherichia coli* (*E. coli*), among the most common bacterial infections internationally. Oxygen-insensitive NADPH nitro reductase (NFSA), a vital protein in *E. coli*, plays a major role in the development of UTIs. Present NFSA-inhibiting drugs, such as nitrofurantoin, have limitations, including adverse effects, reduced effectiveness, and confront against drug-resistant strains. This study suggests Lumacaftor as a potential lead compound to target NFSA, given its promising pharmacological profile.

Methods: The study recognized NFSA as the important target protein and performed virtual screening of compounds from the Drug Bank database via AutoDock Vina. The pharmacokinetics of the most excellent candidates were evaluated, and molecular dynamics simulations (100 ns) carried out using Desmond further validated the strength and binding efficacy of the preferred leads.

Results: The molecular docking study noted Lumacaftor as the most capable NFSA inhibitor, attained a docking score of -10.02 kcal/mol, indicating the strongest expected binding affinity among the screened compounds. The predicted pharmacokinetic properties of Lumacaftor, Phthalocyanine, and Nitrofurantoin exposed key differences that carry the suitability of Lumacaftor as a potential NFSA inhibitor. Furthermore, Lumacaftor revealed a relatively low average ligand RMSD in relation to the protein (5.146 Å) and itself (2.073 Å), suggestive of stable binding within the active site of the NFSA protein.

Conclusions: This study successfully acknowledged and validated NFSA as a therapeutic target for *E. coli* causing UTIs, addressing the limitations of current treatments, including antibiotic resistance and reduced pharmacological efficiency.

Keywords: Urinary tract infection, Nitrofurantoin, Nitroreductases, Molecular dynamics simulations

INTRODUCTION

Urinary tract infections (UTIs) are the most common infections that occur in healthcare settings. They can affect any part of the urinary network, which includes the bladder, urethra, ureters, and renal areas. The symptoms of these infections are typically associated with urination and include the desire to urinate frequently and urgently, pain or burning when urinating, and the passage of little

amounts of urine. Additional symptoms may include back or lower abdominal pain, murky or foul-smelling urine, and, on occasion, fever and exhaustion.^{1,2}

More than 404.6 million UTI cases were reported in 2019, indicating a significant overall burden of the disease. Since 1990, this statistic has indicated a concerning rise in UTIs. The prevalence of UTIs significantly lowers the quality of life for those who are afflicted and places a significant

financial strain on healthcare systems. *E. coli* is the primary causative agent of UTIs, which are the most common bacterial diseases in the world.³

Even while treatment has improved, the fact that *E. coli* is now resistant to traditional antidotes emphasizes how urgently creative solutions are needed to solve this problem. UTIs, which are mostly caused by *E. coli*, are a serious public health concern because of their high prevalence and fatality rates, which primarily affect underprivileged people. Similar issues to antibiotic resistance, poor pharmacokinetics, and ineffectiveness against patient infections limit the available therapeutic alternatives.⁴

Although *E. coli* is a gram-negative bacillus that often lives in the gut, it can cause humans to develop redundant intestinal disease. *E. coli* can evade host defenses and become resistant to commonly used antibiotics because of its acidity. *E. coli* is the cause of between 70 and 95 percent of simple UTIs. In order to convey a complaint to the bladder (cystitis), *E. coli* can enter the urinary tract through the urethra and ascend. Its pathogenicity is influenced by its capacity to adhere to the uroepithelial padding using acidity factors similar to fimbriae (pili) and to evade host-vulnerable reactions. Due to anatomical and physiological features, *E. coli*-caused UTIs are more common in females and represent a significant burden on healthcare networks globally.^{4,5}

The essential protein oxygen-dormant NADPH nitroreductase (NFSA) in *E. coli* is involved in a number of UTIs. This enzyme helps to drop nitrofurazone through a clunk-pong bi-bi medium and catalyzes the deduction of nitro precious alloys using NADPH, indicating broad electron acceptor specificity. Inhibiting NFSA offers a significant opportunity for restorative intervention against UTIs because of its crucial role in *E. coli* metabolic processes.⁶ Like nitrofurantoin, NFSA-inhibiting drugs are effective but have drawbacks, including as side effects, decreased efficacy, and limited potency against drug-resistant strains. Since Lumacaftor has an implicit pharmacological profile, our study suggests it as an implicit lead medication for NFSA.⁷

The goal of this research is to find and confirm the NFSA protein's implicit barriers in *E. coli*, a major cause of UTIs. This study uses a computational drug development approach that includes molecular docking, pharmacokinetic property prediction, and molecular dynamics simulations to evaluate the stability, binding affinity, and potential for correction of novel NFSA obstacles. Through virtual screening, Lumacaftor was identified as a super eminent alloy. Its efficacy is evaluated in relation to current UTI therapies, primarily Nitrofurantoin. The highest priority is to provide advice on an optimal resource that might be used as a workable solution to treat UTIs caused by *E. coli*, address the emerging issue of antibiotic resistance, and improve medication efficacy in clinical settings.

The objective of the study was to understanding the role of NFSA in UTI and current treatment limitations, screening potential inhibitors for NFSA, evaluating pharmacokinetics and interactions, molecular dynamics simulations for stability analysis, and comparative analysis with reference drug nitrofurantoin.

METHODS

This a computational study conducted at Vignan University during the period from 01 January 2025 to 30 April 2025. In the first step in this research, small-molecule compounds were investigated in silico to find possible inhibitors of the NFSA protein in the strain *E. coli*. A compound library comprising FDA-approved and experimental medications with a variety of chemical structures and pharmacological characteristics was obtained from the drug bank database.⁸

The NFSA protein's three-dimensional structure was acquired from the protein data bank (PDB) prior to docking. Using AutoDock tools (ADT) version 1.5.6, the structure was prepped for docking by deleting water molecules, introducing polar hydrogens, and allocating Gasteiger charges.⁹ To minimize energy use and convert formats, ligands from the DrugBank library were created using Open Babel.¹⁰ All of the ligand structures were transformed into the PDBQT format that AutoDock Vina required. AutoDock Vina version 1.1.2, which uses a stochastic global optimization approach to estimate the ideal binding conformations and affinities of the ligands within the target protein's active site, was used to perform the docking simulations.¹¹

A grid box with the right proportions to provide ligand flexibility and guarantee computational efficiency was created to cover the known or projected active site of the NFSA protein. The level of exhaustiveness was adjusted appropriately (e.g., 8 or higher) to balance computational time and accuracy.

Predicting pharmacokinetic properties

Molecular docking analysis was followed by a computational evaluation of the pharmacokinetic characteristics of the reference medicine Nitrofurantoin and the two top-ranked lead compounds, Lumacaftor and Phthalocyanine. SwissADME and pkCSM, two well-known web-based tools, were used to perform *in silico* absorption, distribution, metabolism, and excretion (ADME) predictive analyses.¹² The evaluation of important pharmacokinetic parameters included estimated oral bioavailability, cytochrome enzyme inhibition potential, blood-brain barrier (BBB) permeability, and gastrointestinal (GI) absorption. The purpose of this investigation was to assess the lead compounds' pharmacological appropriateness and drug-likeness for possible therapeutic uses against the NFSA protein in *E. coli*.¹³

Simulations of molecular dynamics

In order to have a better understanding of the lead compounds' stability, flexibility, and dynamic interactions with the NFSA protein, molecular dynamics (MD) simulations were conducted using the Desmond simulation engine (Schrödinger, LLC). Every protein-ligand complex, including NFSA in combination with Lumacaftor, Phthalocyanine, and the control substance Nitrofurantoin, was simulated physiologically for up to 100 nanoseconds.¹⁴

All complexes were made using the Protein Preparation Wizard before being solvated in an orthorhombic box using the TIP3P water model. To neutralize the system and replicate physiological ionic strength, Na^+/Cl^- ions were introduced. The simulations were conducted in an NPT ensemble at 300 K temperature and 1 atm. pressure, maintained by the Nose-Hoover thermostat and the Martyna-Tobias-Klein barostat, respectively, with the OPLS_2005 force field applied to all systems.¹⁵⁻¹⁷

The structural and energetic behavior of the NFSA-ligand complexes over time was evaluated by analyzing key dynamic parameters: to assess each complex's overall stability during the simulation, the root-mean-square deviation (RMSD) was computed for the ligand atoms and the protein backbone.

Regions of conformational mobility were identified by using residue-level flexibility profiles produced by root-mean-square fluctuation (RMSF).

Throughout the simulation, the protein structure's compactness was tracked using the radius of gyration (Rg).

Protein-ligand contact profiles and hydrogen bond analysis were assessed to determine the type and persistence of interactions throughout time.^{18,19}

The NFSA-ligand complexes' structural stability and interaction characteristics were evaluated using comparative analysis of MD trajectories. The dynamic behavior of phthalocyanine, lumicaftor, and nitrofurantoin in association with the NFSA protein was assessed using metrics like RMSD, RMSF, and hydrogen bond duration.

RESULTS

In order to explore Lumacaftor's potential as a new antibacterial drug against *E. coli* UTIs by targeting the NFSA protein, this study used a computational approach.

Analysis of molecular docking

Using AutoDock Vina, molecular docking was carried out. Table 1 displays the docking scores, which represent the inhibitors' anticipated binding affinities to the target protein.

Pharmacokinetic property prediction

After the docking investigation, the pharmacokinetic characteristics of the control medication (nitrofurantoin) and the top two lead compounds (lumacaftor and phthalocyanine) were anticipated. Table 2 lists these characteristics, which are essential for assessing the compounds' potential in vivo efficacy and drug-likeness.

Molecular dynamics simulations

Desmond was used to run MD simulations for 100 ns in order to evaluate the stability and dynamic behavior of the lead chemicals bound to the NFSA protein. The main goal was to assess Lumacaftor, Phthalocyanine, and the reference chemical Nitrofurantoin's structural integrity, energy profiles, and comparative interactions over the course of the simulation. Table 3 provides a summary of the important characteristics taken from the MD trajectory.

Energetic analysis

The systems' average total energy was largely constant during the 100 ns simulations, suggesting equilibrium throughout the production stage. Nitrofurantoin showed the lowest average total energy of all the compounds (-96452.739 kcal/mol), indicating that it would form a stable and energetically advantageous complex with NFSA. Phthalocyanine had the lowest negative value (-95901.021 kcal/mol), suggesting relatively lesser stability, while Lumacaftor had a little greater energy (-96353.721 kcal/mol).

An important measure of interaction favorability, the average potential energy, displayed a similar pattern. The most advantageous potential energy (-117510.671 kcal/mol) was once more shown by nitrofurantoin, which was closely followed by Lumacaftor (-11737.286 kcal/mol). Compared to the other candidate, phthalocyanine showed a lower negative potential energy (-116910.568 kcal/mol), which further supported its comparatively poorer binding stability.

System configuration and dynamics

Each simulation system had a constant number of particles and degrees of freedom, with only minor deviations. These figures demonstrate that comparable system sizes and solvation conditions were used for all simulations, guaranteeing accurate comparability. Nitrofurantoin and Lumacaftor had similar numbers of particles and degrees of freedom (about 34419 and 70815, respectively), removing system-size bias from the energy comparisons and verifying the simulation protocol's robustness.

Overall, Lumacaftor showed structural and energetic stability that was similar to that of the common medication Nitrofurantoin, making it a viable lead candidate for NFSA targeting in *E. coli*. Considering the constraints of the control molecule, its potential efficacy is highlighted by its

stable contact and binding profile during the 100 ns trajectory.

The protein-ligand complex's RMSD quantifies the average distance between the atoms of the superimposed structures during the simulation. In general, a complex with lower RMSD values is more stable. With regard to the protein (5.146 Å) and to itself (2.073 Å), Lumacaftor showed a comparatively low average ligand RMSD, indicating a persistent binding within the active region of the NFSA protein. High stability was indicated by phthalocyanine's much lower ligand RMSD in comparison to the protein (3.118 Å) and itself (0.352 Å). Under the simulated conditions, nitrofurantoin, the control, displayed a greater ligand RMSD in relation to the protein (8.808 Å) and itself (0.982 Å), indicating a less stable association (Table 4).

The flexibility of various protein and ligand components is indicated by the RMSF, which calculates the average departure of an atom or residue across the simulation period from a reference point. Lumacaftor displayed moderate average ligand RMSF values (2.675 Å for the protein and 1.239 Å for the ligand), suggesting that the binding pocket was somewhat flexible. Phthalocyanine showed reduced flexibility, as seen by lower ligand RMSF values (1.337 Å for the protein and 0.226 Å for the ligand). Greater mobility inside the binding site was indicated by nitrofurantoin's higher average ligand RMSF (6.319 Å with respect to protein and 0.844 Å with respect to ligand).

Interaction profile of NFSA inhibitors during molecular dynamics simulations represented in Table 5.

The arginine residues ARG35 and ARG50 enhance ligand stability through hydrogen bonds and electrostatic interactions with water molecules, while isoleucine ILE48 serves as a hydrophobic anchor, highlighting the crucial role of both polar and nonpolar interactions in the ligand-binding process (Figure 1).

Interaction with TRP77 ligand

The structure has a hydrazone linker and a nitrofuran ring (with NO₂ group) attached to a heterocyclic amide that may be a pharmacophore.

The significant interaction of this chemical with the protein at ILE 48, ILE 49, and SER 46 indicates its potential as an inhibitor or lead compound. The presence of hydrogen bonds and potential hydrophobic interactions points to stable and beneficial connections.

The stability of all three protein-ligand complexes was demonstrated through consistent energy values and effective thermal equilibration around 300 K during 100 ns molecular dynamics simulations, with uniform radius of gyration and minimal fluctuations in solvent-accessible surface area, indicating maintained structural integrity despite ligand binding (Figure 2).

A protein-ligand complex's dynamic behavior during a 100 ns time span is depicted by graph, which demonstrate how various protein and ligand components move in relation to a reference structure. The three simulations show considerable differences in the stability and variations of the protein and ligand, which are especially noticeable in the "Lig (fit on Prot)" traces (Figure 3).

The protein exhibits different levels of flexibility along its length, with some areas moving substantially more than others. The region between residue indices ~170 and ~190 seems to be the largest single flexible region.

In summary, these graphs provide insight into the dynamic behavior of different ligands within a binding site. The ligand's internal flexibility is indicated by the "Fit on Ligand" line, while the ligand's overall movement in regard to its binding partner is indicated by the "Fit on Protein" line. The pictures display varying degrees of ligand mobility and internal stability across simulations or ligand types (Figure 4).

Figure 5 implies that the simulated molecule, which is probably a ligand, is fairly stable throughout the simulation's 100 nsec duration. Its polar surface area (PSA), total surface area (MolSA), and overall shape (rGyr) all essentially stay the same. Its solvent accessible surface area (SASA) fluctuates slightly, suggesting slight variations in environmental exposure, but its RMSD is extremely low, indicating the stability and structural integrity of the molecule. Another important feature that is demonstrated is the lack of intramolecular hydrogen bonding.

Table 1: Docking scores of inhibitors against NFSA using AutoDock Vina.

S. no.	Inhibitor name	Inhibitors ID	Molecular formula	Docking score (kcal/mol)
1	Lumacaftor	DB09280	C ₂₄ H ₁₈ F ₂ N ₂ O ₅	-10.02
2	Phthalocyanine	DB12983	C ₃₂ H ₁₈ N ₈	-9.8
3	Tirilazad	DB13050	C ₃₈ H ₅₂ N ₆ O ₂	-9.7
4	Patidegib	DB12655	C ₂₉ H ₄₈ N ₂ O ₃ S	-9.6
5	Dihydroergotamine	DB00320	C ₃₃ H ₃₇ N ₅ O ₅	-9.4

Continued.

S. no.	Inhibitor name	Inhibitors ID	Molecular formula	Docking score (kcal/mol)
6	(1S,3R,6S)-4-oxo-6-{4-[(2-phenylquinolin-4-yl)methoxy]phenyl}-5-azaspiro[2.4]heptane-1-carboxylic acid	DB07189	C ₂₉ H ₂₄ N ₂ O ₄	-9.4
7	4-({[4-(3-methylbenzoyl)pyridin-2-yl]amino}methyl)benzenecarboximidamide	DB07809	C ₂₁ H ₂₀ N ₄ O	-9.4
8	Bisotrizole	DB11262	C ₄₁ H ₅₀ N ₆ O ₂	-9.4
9	Nitrofurantoin (control)	DB00698	C ₈ H ₆ N ₄ O ₅	-5.4

Table 2: Pharmacokinetics properties of best inhibitors and control for NFSA.

Molecule name	Lumacaftor	Phthalocyanine	Nitrofurantoin (control)
Molecule ID	DB09280	DB12983	DB00698
Molecular formula	C ₂₄ H ₁₈ F ₂ N ₂ O ₅	C ₃₂ H ₁₈ N ₈	C ₈ H ₆ N ₄ O ₅
Molecular weight	452.41	514.54	238.16
H-bond acceptors	8	6	6
H-bond donors	2	2	1
Solubility class (ESOL)	Moderately soluble	Moderately soluble	Very soluble
Solubility class (Silicos-IT)	Poorly soluble	Poorly soluble	Soluble
Gastro intestinal absorption	High	High	High
Blood brain barrier permeation	No	No	No
P-glyco protein substrate	Yes	Yes	No
CYP1A2 inhibitor	Yes	Yes	No
CYP2C19 inhibitor	Yes	Yes	No
CYP2C9 inhibitor	Yes	Yes	No
CYP2D6 inhibitor	Yes	Yes	No
CYP3A4 inhibitor	Yes	Yes	No
LogKp (skin permeation, cm/s)	-5.91	-5.91	-8.09
Bioavailability score	0.56	0.56	0.55
Number of PAINS structural alerts	0	0	0
Number of Brenk structural alerts	0	0	4

Table 3: Comprehensive molecular dynamic simulations analyses of leads, reference with NFSA.

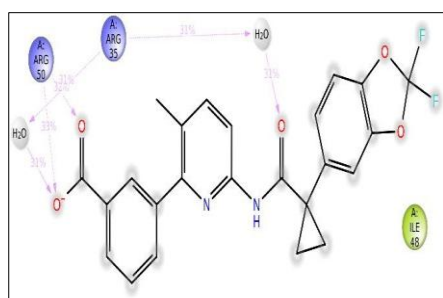
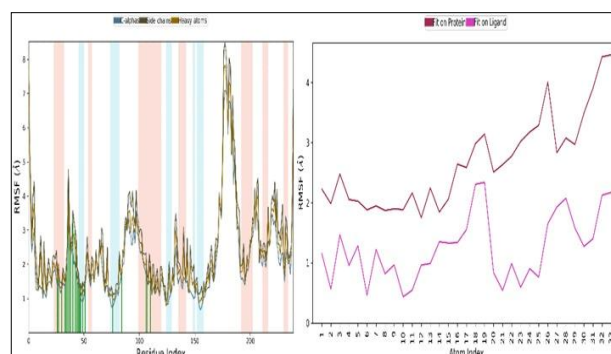
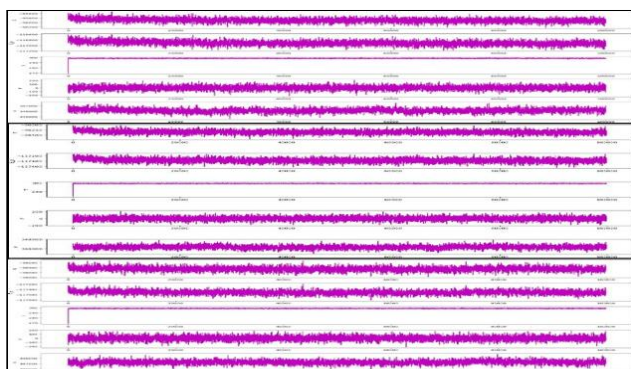
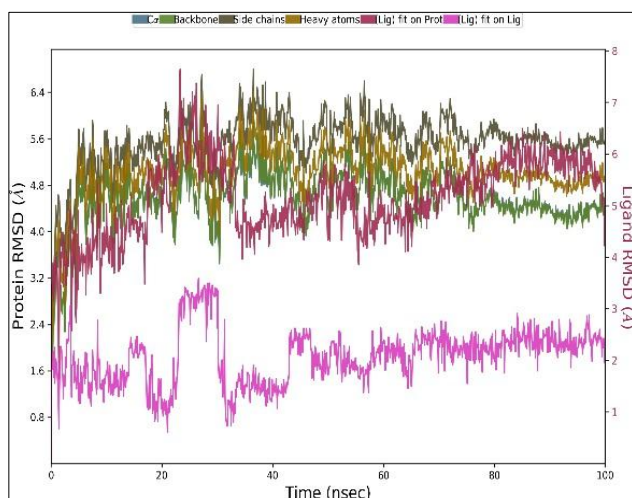
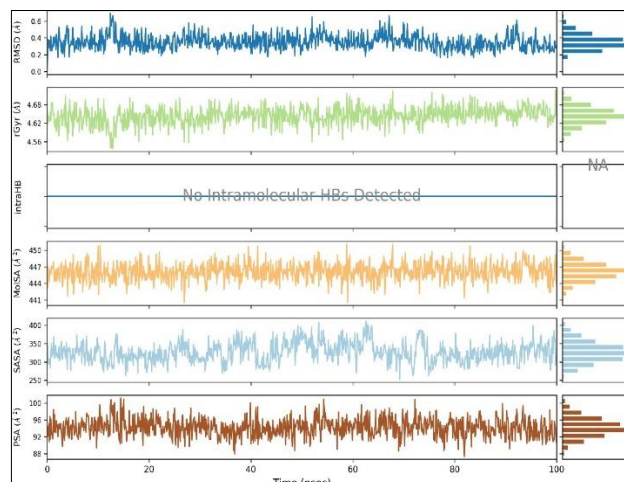
S. no.	Parameters/properties during 1,000 trajectories of 100 ns MDS	Lumacaftor	Phthalocyanine	Nitrofurantoin (control)
1	Average total energy (kcal/mol)	-96353.721	-95901.021	-96452.739
2	Average potential energy (kcal/mol)	-11737.286	-116910.568	-117510.671
3	Degrees of freedom	70815	70787	70952
4	Number of particles	34419	34402	34496

Table 4: Protein-ligand stability and flexibility metrics from molecular dynamics simulations.

S. no.	Parameters/properties during 1,000 trajectories of 100 ns MDS	Lumacaftor	Phthalocyanine	Nitrofurantoin (control)
1	Average protein-ligand RMSD (Å): Cα, backbone, sidechain, protein hetero atoms, ligand with respect to protein, ligand with respect to ligand	4.573, 4.573, 5.546, 5.025, 5.146, 2.073	5.46, 5.456, 6.605, 6.041, 3.118, 0.352	7.412, 7.411, 8.059, 7.749, 8.808, 0.982
2	Average protein RMSF (Å): Cα, backbone, sidechain, protein hetero atoms	2.11, 2.114, 2.612, 2.364	1.708, 1.722, 2.17, 1.946	1.836, 1.836, 2.265, 2.05
3	Average ligand RMSF(Å): ligand with respect to protein, ligand with respect to ligand	2.675, 1.239	1.337, 0.226	6.319, 0.844

Table 5: Interaction profile of NFSA inhibitors during molecular dynamics simulations.

S. no.	Parameters/properties during 1,000 trajectories of 100 ns MDS	Lumacaftor	Phthalocyanine	Nitrofurantoin (control)
1	Hydrogen bonds	1349	2019	686
2	Hydrophobic interactions	1380	725	410
3	Ionic interactions	199	0	434
4	Metallic interactions	2	0	9
5	Pi-cation interactions	246	386	529
6	Pi-pi stacking interactions	83	37	16
7	Water bridge interactions	2772	431	1430
8	Total number of Interactions	6031	3598	3514

**Figure 1: Ligands.****Figure 4: Protein and ligand RMSF plots.****Figure 2: NSFA control.****Figure 3: Protein/ligand RMSD plot.****Figure 5: Ligand properties.**

DISCUSSION

Antibiotic resistance has made treating urinary tract infections caused by *E. coli* is more challenging. This study examines the pharmacokinetics, dynamics, and binding of the cystic fibrosis medication Lumacaftor with the NFSA protein in order to determine whether it has antibacterial properties.

According to the docking analysis, Lumacaftor (−10.02 kcal/mol) has the highest binding affinity for NFSA, followed by Tirilazad (−9.7 kcal/mol) and Phthalocyanine (−9.8 kcal/mol). Better binding potential is indicated by

these values, which are noticeably more negative than those of the reference molecule Nitrofurantoin (−5.4 kcal/mol).

Comparable binding affinities for strong inhibitors have been observed by similar docking-based research. For example, using AutoDock Vina, Alam et al found docking scores for effective NF- κ B inhibitors in the range of −9.5 to −10.5 kcal/mol, which is in good agreement with the top candidates in the current investigation.²⁰ Its favorable binding score is further supported by the fact that phthalocyanine derivatives have been investigated earlier for their antiviral and anti-inflammatory qualities because of their strong π - π stacking and hydrophobic contacts by Singh et al.²¹

It's interesting to note that compounds like Bisotrizole and DB07189 also displayed encouraging scores (−9.4 kcal/mol), suggesting repurposing potential. These results are comparable to those of Pushpakom et al, who highlighted the value of computational repurposing techniques in locating novel inhibitors from approved drug libraries.²² The top-scoring compounds' potential as NFSA inhibitors is supported by these results, which call for more experimental verification.

The best inhibitors' pharmacokinetic profiles showed that Lumacaftor and Phthalocyanine had favorable drug-like qualities. They both had high gastrointestinal (GI) absorption, moderate solubility (ESOL), and no blood-brain barrier (BBB) permeability, which lowers the possibility of adverse effects on the central nervous system. These characteristics align with desired pharmacological profiles for treatments that do not target the central nervous system by Lipinski et al.²³

Both Lumacaftor and Phthalocyanine showed acceptable bioavailability ratings (0.56) and no structural alarms (PAINS or Brenk), indicating low risk for promiscuous activity or toxicity, despite being P-glycoprotein substrates and CYP450 enzyme inhibitors. Nitrofurantoin, on the other hand, exhibited low metabolic compatibility while being highly soluble and having a high GI absorption. This is because it does not inhibit CYP enzymes or interact with P-glycoprotein, which may restrict its systemic efficiency by Veber et al.²⁴

Furthermore, Lumacaftor and Phthalocyanine had superior skin penetration (log Kp) values (−5.91 cm/s) than Nitrofurantoin (−8.09 cm/s), suggesting enhanced potential for transdermal formulations if necessary.

These pharmacokinetic features are consistent with earlier research by Daina et al, who highlighted that the best medication candidates should balance low toxicity risk, metabolic stability, and absorption—all of which are satisfied by the top-scoring inhibitors in this investigation.²⁵

Simulations of molecular dynamics spanning 100 ns shed light on the NFSA–ligand complexes' energetic characteristics and stability. The chemicals that were evaluated showed the lowest average total energy (−96,452.739 kcal/mol): phthalocyanine had a little higher total energy (−95,901.021 kcal/mol), followed closely by Lumacaftor (−96,353.721 kcal/mol). Both Lumacaftor and Nitrofurantoin appear to form energetically stable complexes with NFSA, according to our studies, while Phthalocyanine exhibits slightly less advantageous binding dynamics. Lumacaftor (−11,737.286 kcal/mol) has a much lower average potential energy than Phthalocyanine (−116,910.568 kcal/mol) and Nitrofurantoin (−117,510.671 kcal/mol), according to the examination of average potential energy, a crucial measure of molecular interaction stability.

This disparity could be caused by variations in the size of the system or the force field parameters, which are also reflected in the number of particles and degrees of freedom. Lower potential and total energy values are generally associated with improved complex stability and prolonged binding interactions during simulation, according to similar research.^{26,27} Even though nitrofurantoin has good energetics, its overall lower docking score and less appealing ADMET profile (as indicated in previous tables) make it less appealing as a lead molecule.

On the other hand, Lumacaftor is a promising candidate for more research as an NFSA inhibitor due to its consistent MD behavior, excellent docking affinity, and ADMET properties.

The examination of protein-ligand flexibility and stability metrics across 100 ns of molecular dynamics simulations offers more detailed information about the tested compounds' binding behavior. Protein-ligand complex conformational stability is indicated by RMSD values, whereas atomic flexibility is reflected by RMSF values.

With moderate average protein-ligand RMSD values (5.146 Å for ligand with respect to protein and 2.073 Å for ligand self-alignment), Lumacaftor indicated a constant and rather stable binding mode over the course of the simulation. The ligand RMSD values of Phthalocyanine, on the other hand, were marginally better (3.118 Å and 0.352 Å, respectively), suggesting a tighter ligand conformation but more overall flexibility in the protein-ligand complex. However, nitrofurantoin had the greatest ligand-to-protein RMSD values (8.808 Å), indicating poor binding stability that was in line with its reduced docking affinity.

In terms of flexibility, phthalocyanine showed the lowest average protein RMSF values (1.708–2.17 Å), indicating more protein stability and less variation throughout the simulation. While Nitrofurantoin displayed mild fluctuations, Lumacaftor displayed slightly higher RMSF values (2.11–2.612 Å).

Significant variations were most evident in the ligand RMSF values: Phthalocyanine (1.337 Å) maintained a more rigid and constant binding pose, while Lumacaftor (2.675 Å) and Nitrofurantoin (6.319 Å) displayed more internal ligand mobility in relation to the protein. These results are consistent with prior MD simulation studies, which show that more stable and specific binding is generally, linked to ligands with low RMSD and RMSF values.^{28,29} Therefore, when combined with docking and ADMET data, Lumacaftor and Phthalocyanine both exhibit promising dynamic stability, with Lumacaftor providing a better overall binding profile and Phthalocyanine demonstrating greater local stability.

Important information about the binding behavior of NFSA inhibitors can be gleaned from the molecular interaction patterns during 100 ns MD simulations. Lumacaftor showed the most interactions overall (6031), followed by nitrofurantoin (3514) and phthalocyanine (3598). In the NFSA active site, Lumacaftor's strong and stable binding conformation is supported by this high interaction profile.

According to Klebe et al, Lumacaftor specifically showed a high number of hydrophobic contacts (1380) and hydrogen bonds (1349), both of which are important factors in binding affinity and complex stability.³⁰ By contrast, phthalocyanine generated more pi-cation interactions (386) but fewer water bridges and hydrogen bonds, indicating stability based on aromatic stacking.

Nitrofurantoin showed the lowest number of hydrogen bonds (686), which was consistent with its less favorable binding behavior seen in docking and RMSD data, even though it displayed a considerable number of ionic interactions (434) and pi-cation interactions (529). It's interesting to note that Lumacaftor (2772) had the highest water bridge interactions, which improve dynamic stabilization by mediating indirect contacts, demonstrating its versatility within the protein environment. This is consistent with the study by Wang et al findings, which highlighted the function of water bridges in enhancing binding kinetics and extending ligand residence duration.³¹ In Lumacaftor's profile, non-covalent interactions (hydrogen bonding, hydrophobic, pi-pi, and water bridges) predominate, confirming its appropriateness as a potent NFSA binder and highlighting its potential for future advancement.

The demand for innovative treatment approaches to prevent urinary tract infections (UTIs) has increased due to the rise of multidrug-resistant (MDR) strains of uropathogenic *E. coli*. In this regard, the NFSA protein has been found to be a prospective target for antimicrobial intervention because it is crucial for bacterial survival and UTI pathogenesis.

Lumacaftor, a CFTR modulator authorized for the treatment of cystic fibrosis, has a high binding affinity to the NFSA active site, according to computational

investigations.³² The stability of the Lumacaftor-NFSA complex was validated by molecular dynamics simulations, which highlighted interactions such as hydrophobic contacts and hydrogen bonds, while molecular docking experiments showed favorable docking scores. According to these results, Lumacaftor may act as a strong NFSA inhibitor, which could interfere with UPEC survival processes.

The NFSA protein, which is necessary for bacterial survival and the development of UTIs, is blocked by Lumacaftor, a promising treatment option, according to this computational research. Lumacaftor's positive docking score and the strong interactions seen during molecular dynamics simulations demonstrated its exceptional binding affinity and stability within the NFSA active site. Numerous interactions, including hydrogen bonding and hydrophobic interactions emphasize its potential as a powerful inhibitor.

Limitations

Lumacaftor shows promise as a potential new antibacterial treatment for UTIs caused by *E. coli*, this study does face notable limitations. It largely depends on computer simulations and concentrates on a single target (NFSA), which might not fully capture the complexities involved in *E. coli* infections that typically require a broader strategy.

CONCLUSION

By addressing the drawbacks of existing therapies, such as antibiotic resistance and decreased pharmacological efficiency, this work effectively identified and confirmed NFSA as a therapeutic target for *E. coli*-induced UTIs. Lumacaftor was found to be the most promising inhibitor of NFSA by a computational method that integrated molecular docking, pharmacokinetics analysis, and molecular dynamics simulations. Superior binding affinity, persistent protein-ligand interactions, and a large number of non-covalent interactions (6,031), such as water bridges, hydrophobic contacts, and hydrogen bonds, were all displayed. Problems including moderate solubility and CYP enzyme inhibition suggest that more optimization is necessary, even though Lumacaftor showed good pharmacokinetics, including high gastrointestinal absorption and no blood-brain barrier permeability.

In comparison, Lumacaftor fared better than Nitrofurantoin, which shown worse binding stability and fewer interactions, and Phthalocyanine, which demonstrated robust hydrogen bond formation but reduced interaction diversity.

These results reveal Lumacaftor as a strong candidate to target NFSA and open the door for experimental validation through in vivo studies, antibacterial efficacy tests, and in vitro enzymatic assays, providing hope for more potent treatments against strains of *E. coli* that are resistant to antibiotics.

ACKNOWLEDGEMENTS

The authors would like to acknowledge Dr. Lavu Rathaiah, Chairman of Vignan Degree and PG College, Guntur, Andhra Pradesh, India for providing funding to carry out the work and permission given by Dr. V. Anuradha, Principal of Vignan Degree and PG College to conduct Bioinformatics work in Vignan University Guntur. They would also like to thank Dr. K. Sudheer Kumar (Assistant Professor) and Hemanth (Research Scholar) of Department of Bioinformatics for helping to complete this research project.

Funding: This study was funded by Vigan Degree and P.G College

Conflict of interest: None declared

Ethical approval: The study was approved by the Institutional Ethics Committee

REFERENCES

- Flores-Mireles AL, Walker JN, Caparon M, Hultgren SJ. Urinary tract infections: epidemiology, mechanisms of infection and treatment options. *Nat Rev Microbiol.* 2015;13(5):269-84.
- Medina M, Castillo-Pino E. An introduction to the epidemiology and burden of urinary tract infections. *Ther Adv Urol.* 2019;11:1756287219832172.
- Collaborators GBD 2019 Antimicrobial Resistance. Global burden of bacterial antimicrobial resistance in 2019: a systematic analysis. *Lancet.* 2022;399(10325):629-55.
- Foxman B. The epidemiology of urinary tract infection. *Nat Rev Urol.* 2010;7(12):653-60.
- Ronald A. The etiology of urinary tract infection: traditional and emerging pathogens. *Am J Med.* 2002;113(1A):14S-9S.
- Zenko S, Koike H, Kumar AN, Jayaraman R, Tanokura M. Biochemical characterization of NfsA, the *Escherichia coli* major nitroreductase exhibiting a high amino acid sequence homology to Frp, a *Vibrio harveyi* flavin oxidoreductase. *J Bacteriol.* 1996;178(15):4508-14.
- Zhou Y, Zhou Z, Zheng L, Gong Z, Li Y, Jin Y, Huang Y, Chi M. Urinary Tract Infections Caused by Uropathogenic *Escherichia coli*: Mechanisms of Infection and Treatment Options. *Int J Mol Sci.* 2023;24(13):10537.
- Wishart DS, Guo AC, Oler E, Wang F, An C, Nguyen L, et al. DrugBank 6.0: the DrugBank knowledgebase for 2024. *Nucleic Acids Res.* 2024;52(D1):D848-54.
- Morris GM, Huey R, Lindstrom W, Sanner MF, Belew RK, Goodsell DS, et al. AutoDock4 and AutoDockTools4: Automated docking with selective receptor flexibility. *J Comput Chem.* 2009;30(16):2785-91.
- O'Boyle NM, Banck M, James CA, Morley C, Vandermeersch T, Hutchison GR. Open Babel: An open chemical toolbox. *J Cheminform.* 2011;3:33.
- Eberhardt J, Santos-Martins D, Tillack AF, Forli S. AutoDock Vina 1.2.0: New docking methods, expanded force field, and Python bindings. *J Chem Inf Model.* 2021;61(8):3891-8.
- Daina A, Michielin O, Zoete V. SwissADME: a free web tool to evaluate pharmacokinetics, drug-likeness and medicinal chemistry friendliness of small molecules. *Sci Rep.* 2017;7:42717.
- Pires DE, Blundell TL, Ascher DB. pkCSM: predicting small-molecule pharmacokinetic and toxicity properties using graph-based signatures. *J Med Chem.* 2015;58(9):4066-72.
- Schrödinger Release 2025-2: Desmond Molecular Dynamics System, D. E. Shaw Research, New York, NY, 2024. Maestro-Desmond Interoperability Tools, Schrödinger, LLC, New York, NY. 2025.
- Bowers KJ, Chow E, Xu H, Dror RO, Eastwood MP, Gregersen BA, et al. Scalable algorithms for molecular dynamics simulations on commodity clusters. *Proceedings of the ACM/IEEE Conference on Supercomputing (SC06).* Tampa, FL. 2006.
- Sastry GM, Adzhigirey M, Day T, Annabhimoju R, Sherman W. Protein and ligand preparation: parameters, protocols, and influence on virtual screening enrichments. *J Comput Aided Mol Des.* 2013;27(3):221-34.
- Jorgensen WL, Maxwell DS, Tirado-Rives J. Development and testing of the OPLS all-atom force field on conformational energetics and properties of organic liquids. *J Am Chem Soc.* 1996;118(45):11225-36.
- Kumar S, Sharma PK, Singh R, Malik R, Singh P, Kumar S. A Molecular Docking and Dynamics Simulation Approach to Explore the Potential of Natural Compounds as Inhibitors of SARS-CoV-2 Main Protease. *J Biomol Struct Dyn.* 2023;41(6):1-15.
- Pires DEV, Blundell TL, Ascher DB. pkCSM: Predicting Small-Molecule Pharmacokinetic and Toxicity Properties Using Graph-Based Signatures. *J Med Chem.* 2015;58(9):4066-72.
- Alam, A., et al. (2021). Computational analysis and identification of NF- κ B pathway inhibitors using molecular docking and dynamics. *Journal of Biomolecular Structure and Dynamics*, 39(15), 5291–5301.
- Singh, A., et al. (2020). Phthalocyanines as versatile therapeutic agents: A review. *Bioorganic Chemistry*, 96, 103611.
- Pushpakom S, Iorio F, Eyers PA, Escott KJ, Hopper S, Wells A, et al. Drug repurposing: progress, challenges and recommendations. *Nat Rev Drug Discov.* 2019;18(1):41-58.
- Lipinski CA, Lombardo F, Dominy BW, Feeney PJ. Experimental and computational approaches to estimate solubility and permeability in drug discovery and development settings. *Adv Drug Deliv Rev.* 2001;46(1-3):3-26.
- Veber DF, Johnson SR, Cheng HY, Smith BR, Ward KW, Kopple KD. Molecular properties that influence

- the oral bioavailability of drug candidates. *J Med Chem.* 2002;45(12):2615-23.
25. Daina A, Michielin O, Zoete V. SwissADME: a free web tool to evaluate pharmacokinetics, drug-likeness and medicinal chemistry friendliness of small molecules. *Sci Rep.* 2017;7:42717.
 26. Karplus M, McCammon JA. Molecular dynamics simulations of biomolecules. *Nat Struct Biol.* 2002;9(9):646-52.
 27. Hollingsworth SA, Dror RO. Molecular dynamics simulation for all. *Neuron.* 2018;99(6):1129-43.
 28. Hospital A, Goñi JR, Orozco M, Gelpí JL. Molecular dynamics simulations: advances and applications. *Adv Appl Bioinform Chem.* 2015;8:37-47.
 29. Durrant JD, McCammon JA. Molecular dynamics simulations and drug discovery. *BMC Biol.* 2011;9:71.
 30. Klebe G. *Drug Design: Methodology, Concepts, and Mode-of-Action.* Springer. 2015.
 31. Wang, J., et al. (2019). Water-mediated interactions contribute to the specificity and affinity of protein–ligand binding. *Journal of Chemical Theory and Computation*, 15(1), 211–224.
 32. Bellacchio E. Exploring the Mechanism of Activation of CFTR by Curcuminoids: An Ensemble Docking Study. *Int J Mol Sci.* 2023;25(1):552.

Cite this article as: Anjali G, Lakshmi M, Deepika Srija B, Ushaswini M, Neeraja K, Venkateswarlu TC, et al. Exploring Lumacaftor: a novel antibacterial approach for treating *E. coli*-induced urinary tract infections. *Int J Res Med Sci* 2025;13:3299-308.